

2<sup>nd</sup> CIRP Conference on Surface Integrity (CSI)

## Biodegradation control of magnesium-calcium biomaterial via adjusting surface integrity by synergistic cutting-burnishing

M. Salahshoor, Y.B. Guo\*

*Dept. of Mechanical Engineering, The University of Alabama, Tuscaloosa, AL 35487, USA*\* Corresponding author. Tel.: +1-205-348-2615; fax: +1-205-348-6419. E-mail address: [yguo@eng.ua.edu](mailto:yguo@eng.ua.edu).**Abstract**

Magnesium-calcium (MgCa) alloys are very promising orthopedic biomaterials with biodegradability and suitable biomechanical properties. However, the high corrosion rate of Mg-based alloys in human body environment remains as a big challenge for their successful development as biomaterials. In this study, synergistic cutting-burnishing was developed to control the degradation rate of the novel MgCa0.8 (wt. %) biomaterial by adjusting surface integrity. In-vitro immersion tests were performed in simulated body fluid to measure degradation kinetics of the processed samples. Morphology and elemental composition of the corroded surface layers were also studied. The synergistic process was successful to control biodegradation rate. This enabling process may manufacture biodegradable MgCa0.8 implants with tailored degradation rate to fit various orthopedic applications.

© 2014 The Authors. Published by Elsevier B.V. Open access under [CC BY-NC-ND license](https://creativecommons.org/licenses/by-nc-nd/4.0/).Selection and peer-review under responsibility of The International Scientific Committee of the “2nd Conference on Surface Integrity” in the person of the Conference Chair Prof Dragos Axinte [dragos.axinte@nottingham.ac.uk](mailto:dragos.axinte@nottingham.ac.uk)*Keywords:* Magnesium; surface integrity; corrosion; implants**1. Introduction**

Biodegradable magnesium-calcium (MgCa) alloys become very attractive recently particularly in orthopedic applications [1]. Compared to commercial metallic biomaterials, e.g. titanium alloys, stainless steels, and cobalt-chromium alloys, MgCa alloys minimize stress shielding and avoid secondary surgery while providing sufficient strength. However, they have very low corrosion resistance in saline environments such as human body and fast degradation kinetics resulting in a large amount of hydrogen and hydroxide which interfere with metabolic reactions and delay the healing process. Successful development of MgCa alloys as novel biomaterials requires design and fabrication of suitable surface integrity to adjust the degradation rate to match healing rate of the bone trauma and absorption rate of the corrosion by products.

In this study, a noncommercial binary MgCa (0.8 wt%) alloy was made in-house. Synergistic cutting–burnishing was used to process the implant surface.

The effects of process parameters on the degradation kinetics were investigated by immersion corrosion tests in the simulated body fluid (SBF). Morphology and elemental composition of the corroded surfaces were investigated using scanning electron microscopy (SEM) and energy dispersive spectroscopy (EDS). The subsurface microstructure of the corroded surfaces was also studied.

**2. Background on corrosion of MgCa alloys**

There have been some efforts recently to study the corrosion performance of MgCa alloys to identify influential parameters. Kannan and Raman [2] reported the general and pitting corrosion resistance of Ca-containing Mg alloys in m-SBF was significantly improved as compared to the base Mg alloy. For example, AZ91Ca alloy exhibited a five-fold increase in the surface film resistance than AZ91 alloy.

Kirkland et al [3] showed the above the solid solubility limit of ~ 1.34 wt% Ca, the corrosion rate of MgCa alloys increased with Ca content and the corrosion potential became more negative. However,

below the solubility limit, the corrosion rate stayed the same or even slightly decreased with increasing Ca additions. It was also revealed that Ca is a unique alloying addition to Mg for biodegradable implants.

Thomann et al [4] showed a slight increase in corrosion resistance of MgCa0.8 alloy with a magnesium fluoride coating compared to uncoated implants.

Drynda et al [5] showed 0.8 wt% Ca concentration resulting in the minimum degradation rate compared to other Ca contents. MgF<sub>2</sub> coated Mg-Ca alloys showed slower rates and no further dependence on Ca content.

Krause et al [6] reported that MgCa0.8 shows an insufficient initial strength and a fast degradation. Although its ductility was constant during degradation and the degradation products were naturally occurring components of the organism.

Thomann et al [7] showed after 12 months the bone-implant-contact was clearly stronger in MgCa0.8 case than other Mg alloys. However, it degraded faster in pitting corrosion than the uniform corrosion of LAE442 but slow enough to avoid gas bubble generation.

Von Der Höh et al [8] found that MgCa0.8 alloy shows obvious pitting corrosion for threaded cylinders but not for turned and sand-blasted implants. In addition, turned implants showed the best integration into the bone compared to sand-blasted and threaded cylinders.

Wang et al [9] demonstrated that the biodegradation rate of an AZ31 alloy can be significantly reduced by grain refinement produced by mechanical processing. They found the highest degradation rate for SC samples. The degradation rates of the HR and ECAP samples, which were significantly smaller than that for SC material, were rather similar.

Denkena and Lucas [10] showed the corrosion rates of the deep rolled MgCa3.0 surfaces were approximately 100 times slower than the corrosion rates of the turned surfaces. The corrosion resistance was improved until the modified layer was dissolved to the bulk region.

Guo and Sealy [11] have developed a laser shock peening process to induce unique surface integrity characterized by high compressive residual stress and extended strain hardening, which significantly enhanced the corrosion resistance of MgCa0.8 alloy by more than 100 fold in simulated body fluid. Furthermore, corrosion of the peened implants was controllable by varying the laser power and peening overlap ratio.

### 3. Immersion Tests

Cylindrical-shaped samples of MgCa0.8 of 38 mm (dia.) × 12 mm (length) were dry face milled using PCD inserts (ADKW 1505-75RW PDR) at feed 0.2 mm/rev, DoC 0.2 mm and velocity 2000 m/min. A square-shaped area of 24 mm × 24 mm was burnished (SiN ball 12.7 mm dia) after face milling. All the samples were ultrasonically cleaned in ethanol and then dried in a stream of air. Unburnished surfaces of each sample were covered to avoid the exposure to simulated body fluid (SBF) in immersion corrosion tests. Table 1 shows the chemical composition of the applied SBF. Fig. 1 shows the experimental set up. The volume of the SBF in the corrosion cell was 2200 ml and its temperature was maintained at 37 ± 1 °C. The solution was also stirred to keep the temperature and chemical concentration uniform all over the cell. Two sets of immersion tests were performed to study the effects of burnishing feed and pressure on degradation kinetics of MgCa0.8. In the pressure-effect set, there was one reference sample which was only face-milled in addition to three more samples burnished at pressure of 2, 6, and 10 MPa. Likewise, there were four samples in the feed-effect set, a face-milled reference and three burnished samples at the feed of 60, 100, and 200 μm. Each test was run for 300 hours and 500 ml of the solution was replaced with fresh SBF for every 12 hours to account for the fluid exchange of an adult human by urination.

Table 1 Chemical composition of the applied SBF in immersion tests.

Chemical Component	Concentration (mg/l)	Chemical Component	Concentration (mg/l)
NaCl	8000	MgSO <sub>4</sub> ·7H <sub>2</sub> O	200
Glucose	1000	CaCl <sub>2</sub> ·2H <sub>2</sub> O	186
KCl	400	Na <sub>2</sub> HPO <sub>4</sub> ·7H <sub>2</sub> O	90
NaHCO <sub>3</sub>	350	KH <sub>2</sub> PO <sub>4</sub>	60

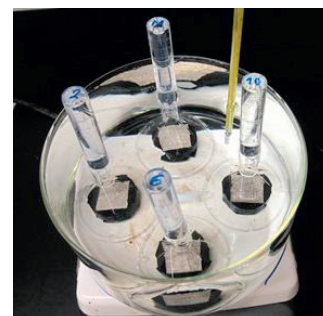
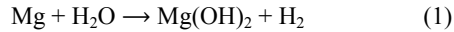


Fig. 1 Immersion corrosion testing setup.

#### 4. Hydrogen Evolution vs. Time

Magnesium reacts very quickly with water, which is plentiful in human body fluid, and produces hydrogen gas and hydroxide according to following reaction:



Based on the stoichiometry in this reaction, oxidation or dissolution of 1 mole magnesium will produce 1 mole hydrogen. Therefore, collecting the evolved hydrogen gas and measuring its volume, eudiometry, in the course of time would be an indirect indication of magnesium degradation kinetics in SBF. Gravimetry is another way to study degradation behavior of magnesium in SBF in which the corroded layer is removed from the samples at certain time intervals and then they are weighed to calculate the amount of mass loss as an indication of degradation kinetics. Eudiometry is easier to implement and more reliable than gravimetry to study long term degradation behavior of magnesium. In the next two sections, eudiometry of hydrogen is used to study the effects of pressure and feed in synergistic cutting-burnishing on in-vitro degradation kinetics of MgCa0.8.

##### 4.1. Burnishing pressure effect on degradation kinetics

Fig. 2 shows the amount of evolved hydrogen collected during 300 hrs. immersion tests on burnished samples processed under different burnishing pressures. It is clear that there is significant improvement in corrosion resistance, particularly in first 100 hrs after implantation, by adding burnishing to the surface layers. The capability to adjust the degradation kinetics of MgCa0.8 alloy, particularly for several days after the surgery, is critical in the sense that absorption rate of the corrosion products could match the production rate in order to avoid accumulation of them in the operation site, disrupting the metabolic reactions, and ultimately delaying healing process. Undisturbed healing will provide bone cells with sufficient time to grow at fractured sites and hence the bone will gain increasingly higher strength for carrying daily life loads as the implant gets weaker due to corrosion.

Imposing surface layers of the MgCa0.8 alloy to synergistic dry cutting-hydrostatic burnishing produces a spectrum of surface integrity starting at the surface and decaying towards the subsurface. Therefore, material layers with different surface integrity and biodegradation properties would be

unveiled as the corrosion progresses and at some point for all the samples, the bulk material with uniform mechanical and biodegradation properties would be attacked by corrosion reaction and that is when the slopes of the plots in Fig. 2 become identical. Higher burnishing pressures show more gain on corrosion resistance which is due to larger and deeper compressive residual stresses in the subsurface [1]. It is worth mentioning that for this set of tests a plastic tape was used to cover the unprocessed surfaces of the samples. It was observed that corrosion had happened on those surfaces as well when the tape was removed at the end of the test. This might have been caused due to crevice corrosion. As the corrosion progresses on target areas of the implants, a narrow gap grows gradually between the surface and the tape which is a potential site for crevice corrosion and it spreads to the rest of the unprocessed surface from there as the time passes on. Therefore, some amount of hydrogen in Fig. 2 is produced by unwanted surfaces; however, since all the samples were in same cell, under same condition, and covered identically the comparative study in Fig. 2 would still be valid. Crevice corrosion is a probable reason that degradation curve corresponding to 6MPa pressure gets ahead of the 2MPa curve after 200 hrs immersion.

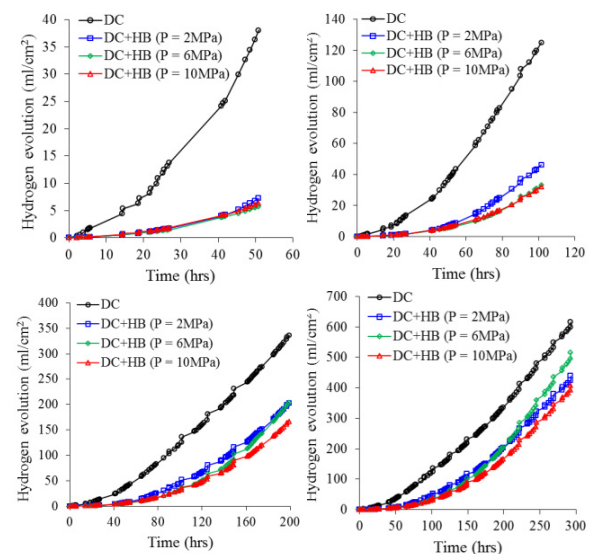


Fig. 2 Effect of burnishing pressure on cumulative hydrogen evolution in 50, 100, 200, and 300 hrs immersion in SBF (DC: dry cutting; HB: hydrostatic burnishing).

The solution temperature and pH were monitored, as are shown in Fig. 3, throughout the immersion test. The temperature was kept around physiological temperature of 37 °C, however, the pH was constantly above the physiological pH of 7.4 even though the solution volume to corroding surface area ratio was

big and almost one quarter of the solution replaced every 12 hrs with fresh solution. The whole solution was replaced by fresh solution at 40<sup>th</sup> hour, seen as a sharp ditch in Fig. 3, to investigate whether there were other unforeseen factors affecting the pH or it was just the fast corrosion reaction producing large amount of hydroxide and rising pH. The pH read-out intervals were selected very short right after the solution replacement and it was noticed that the pH increased fairly quickly and stabilized around 9.65 for the rest of the test. It is expected for degradation to progress faster at physiological pH of 7.4. Higher pH values reflect the presence of larger amount of hydroxide in the solution which will in turn decrease the driving force of the reaction (1) to progress towards the right side and produce more corrosion products. This unconformity in the pH still does not affect the goal of this comparative study to investigate the effect of mechanical surface treatment by synergistic process on degradation kinetics, since all the samples are at same environmental conditions.

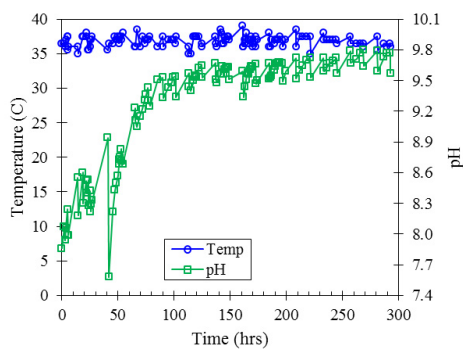


Fig. 3 Time history of solution temp. and pH in pressure-effect test.

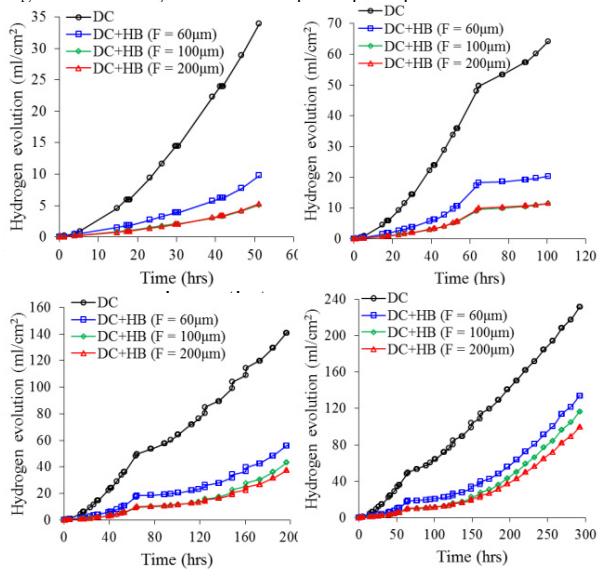


Fig. 4 Effect of feed on cumulative hydrogen evolution in 50, 100, 200, and 300 hrs. immersion in SBF.

in corrosion resistance due to the saturation of compressive residual stress.

To avoid the occurrence of crevice corrosion in this set of samples, the non-processed surface of the samples were covered using nail polisher. However, after about 60 hrs. immersion small particles of nail polish were spotted flowing around in the solution. That was an indication of potential break down in the protective layer in case the test was to run for longer periods. Therefore, the test was stopped and the samples were pulled out of the solution to try cold epoxy mount as the last resort to protect the non-processed surfaces from crevice corrosion. The samples had to be sized smaller in order to fit the epoxy mount molds. That was done by grinding using SiO<sub>2</sub> abrasive papers and the final exposed area was 1.8 mm × 1.8 mm rather than original 2.4 mm × 2.4 mm. The little kink in degradation curves around 60 hr immersion is due to this change in the size of the exposed area. In order to plot the data collected before the cold epoxy mount and afterwards in the same diagram, the measured volume of the collected hydrogen was normalized by the exposed area.

The temperature and pH of the solution were monitored in this test as well (Fig. 5). The temperature was kept around the physiological value; however, the pH showed pretty much the same pattern as in pressure-effect case. The big pH drop in Fig. 5 around 60 hr immersion is caused by replacing the whole solution with fresh one after epoxy mounting of the samples. A longer-term (> 300 hrs.) corrosion test would be helpful to evaluate the limit the process effect.

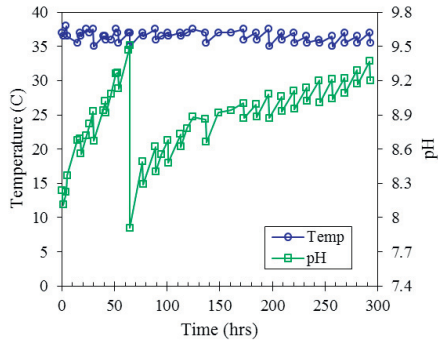


Fig. 5 Time history of solution temp. and pH in feed-effect test.

**5. Surface Morphology and Elemental Composition**

The morphology of the corroded surfaces after immersion tests is shown in Fig. 6. All the samples processed at different burnishing pressures and feeds showed similar morphology with heavily localized corrosion due to the fact that after nearly two weeks of immersion the mechanically affected zone (MAZ) would be dissolved entirely in the solution and underlying substrate would be exposed to corrosive medium. This substrate is the as-cast MgCa0.8 with same mechanical and biodegradation characteristics on all samples. Therefore, degradation will have pretty much the same dynamics on all the samples resulting in similar looking morphology as in Fig. 6.

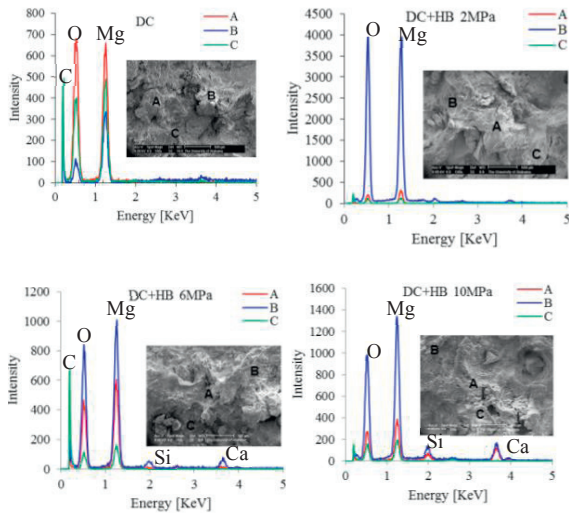


Fig. 6 Surface morphology and EDS spectrum of MgCa0.8 implants processed under different pressure and feed (DC: dry cutting; HB: hydrostatic burnishing).

Energy dispersive spectroscopy (EDS) was also used to investigate the elemental composition of the corroded MgCa0.8 surfaces. Three spots on each sample surface were studied for this purpose and it was noticed that EDS spectrums show different intensities for same energy levels depending on the spot location. This nonhomogeneity in distribution of chemical elements on the corroded surfaces strengthens the notion of localized corrosion. The constituting elements are identified and the average

amount of each element is computed and shown in Fig. 7 for all the samples. Degradation depletes surface layer from Mg, more than 50%, while makes it richer in Ca content. It is also noticeable that more than 50% of the corroded surface layer is composed of oxygen. This could be due to diffusion of phosphate (PO<sub>4</sub>)<sup>3-</sup> and carbonate (CO<sub>3</sub>)<sup>2-</sup> ions from the solution into the surface or hydroxide (OH<sup>-</sup>) formation on the surface. It is worth mentioning here that all sample surfaces were covered with a thick layer of powder-like, white-color substance which was removed mechanically to expose the surfaces shown in Fig. 6. There is a very high chance for this substance to be magnesium hydroxide Mg(OH)<sub>2</sub> particularly due to high pH value of the solution in Figs. 3 and 5 which stabilizes the hydroxide. The other possibility is the formation of hydroxyapatite Ca<sub>10</sub>(PO<sub>4</sub>)<sub>6</sub>(OH)<sub>2</sub> which is the naturally occurring form of calcium and has strong resemblance to the bone structure. This similarity is favored from the medical viewpoint since it stimulates bone cells to grow into the implant surface and make proper bonding which is vital for keeping bone fragments in their original anatomical alignment during recovery.

Characterizing the mentioned substance needs further investigation. Moreover, Si was detected on feed-effect samples as is shown in Fig. 7. This element was neither in the MgCa0.8 alloy nor in the solution (Table 1). A possible source for this element is SiO<sub>2</sub> abrasive papers used in the grinding stage to resize the samples before cold epoxy mounting.

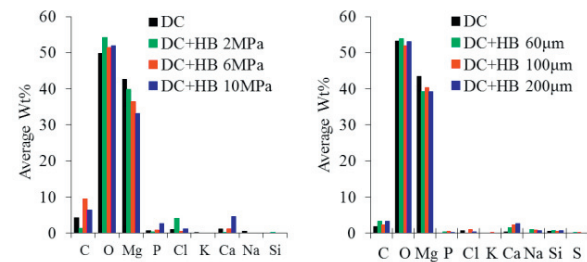


Fig. 7 Quantitative EDS and elemental composition of the corroded MgCa0.8 surfaces (DC: dry cutting; HB: hydrostatic burnishing).

**6. Subsurface Micrographs**

Fig. 8 shows subsurface (cross section) grain sizes of the corroded samples. The localized nature of corrosion after two weeks immersion and irregular shaped pits are clearly visible in the subsurface. The overall reaction (1) consumes H<sup>+</sup> and produces OH<sup>-</sup> which causes the pH value to increase and favors the formation of Mg(OH)<sub>2</sub>. Therefore, it seems the corrosion should stop at some point due to protective function of the formed hydroxide layer. However, in

aqueous physiological solutions which contain chloride (Cl<sup>-</sup>), hydroxide reacts and forms soluble magnesium chloride (MgCl<sub>2</sub>) according to following reaction. This guarantees the degradation of the whole implant until it is completely degraded.



The other factor against complete stabilization of the hydroxide layer is the body fluid flow in actual physiological case. The fluid flow caused by stirring action in the corrosion cell (Fig. 1) accelerates the mass diffusion around implants, prevents the precipitation of corrosion products to some extent, and results in acceleration of Mg<sup>2+</sup> dissolution. The mechanism of the corrosion is complex and is affected by metallurgical factors, alloying additions, and impurities. Mg<sub>2</sub>Ca phase, formed on the grain boundaries, is more active than α-Mg [3] in the bulk of grains and it assumes the role of anode contradicting other intermetallics which are cathode in relation to Mg. Hence, the corrosion concentrates in the grain boundaries followed by undercutting and falling-out of grains. Evidences of such selective attack in grain boundaries are visible in the micrographs of Figs. 8 and 9. This might be a reason for powder-like structure of the white substance mentioned in section 5.

Topographical features, e.g. ridges and grooves, of the burnished and corroded surfaces could give valuable information on the corrosion resistance, which is beyond the scope of this study. This may be a future research subject.

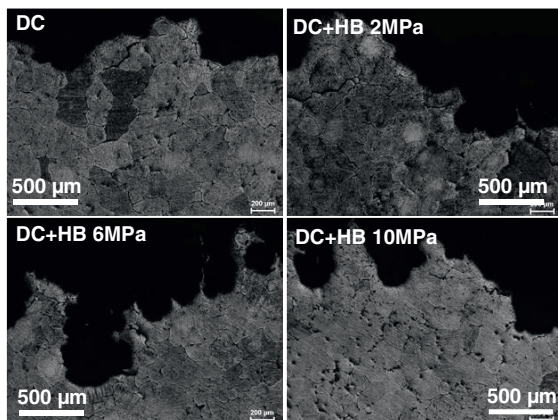


Fig. 8 Subsurface micrographs of the corroded MgCa0.8 surfaces processed under different burnishing pressures (DC: dry cutting; HB: hydrostatic burnishing).

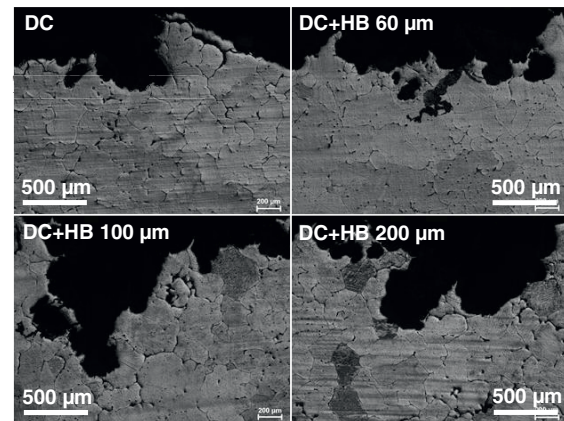


Fig. 9 Subsurface micrographs of the corroded MgCa0.8 surfaces processed under different burnishing feeds (DC: dry cutting; HB: hydrostatic burnishing).

## 7. Conclusions

A novel orthopedic biomaterial MgCa0.8 alloy was processed using the synergistic dry cutting–burnishing. The effect of process parameters on long term degradation behavior of the implants were studied through immersion corrosion tests in SBF. The key results of this study are summarized as follows.

- Synergistic dry cutting–burnishing process is capable of adjusting degradation of the biodegradable MgCa0.8 alloy via tuning surface integrity.
- Higher burnishing pressures and larger feeds result in higher corrosion resistance.
- Long term exposure to corrosive physiological medium will cause the mechanically affected zone to dissolve entirely and the corrosion will happen in more localized fashion afterwards.

## Acknowledgements

The work was supported by NSF CMMI #1000706.

## References

- [1] Guo, Y.B., Salahshoor, M., 2010. Process mechanics and surface integrity by high-speed dry milling of biodegradable magnesium-calcium implant alloys, *CIRP Annals - Manufacturing Technology* 59/1, p. 151.
- [2] Kannan, M.B., Raman, R.K., 2008. In vitro degradation and mechanical integrity of calcium-containing magnesium alloys in modified-simulated body fluid, *Biomaterials* 29, p. 2306.
- [3] Kirkland, N.T., Birbilis, N., Walker, J., Woodfield, T., Dias, G.J., Staiger, M.P., 2010. In-vitro dissolution of magnesium-calcium binary alloys: clarifying the unique role of calcium additions in bioresorbable magnesium implant alloys, *J. Biomedical Materials Research B: Applied Biomaterials* 95, p. 9.
- [4] Thomann, M., Krause, C., Angrisani, N., Bormann, D., Hassel, T., Windhagen, H., Meyer-Lindenberg, A., 2010. Influence of a magnesium-fluoride coating of magnesium-based implants

- (MgCa0.8) on degradation in a rabbit model, *J. of Biomedical Materials Research A* 93, p. 1609.
- [5] Drynda, A., Hassel, T., Hoehn, R., Perz, A., Bach, F.W., Peuster, M., 2010. Development and biocompatibility of a novel corrodible fluoride-coated magnesium-calcium alloy with improved degradation kinetics and adequate mechanical properties for cardiovascular applications, *J. of Biomedical Materials Research A* 93, p. 763.
- [6] Krause, A., Von der Höh, N., Bormann, D., Krause, C., Bach, F.W., Windhagen, H., Meyer-Lindenberg, A., 2010. Degradation behavior and mechanical properties of magnesium implants in rabbit tibiae, *J. of Materials Science* 45, p. 624.
- [7] Thomann, M., Krause, C., Bormann, D., Von der Höh, N., Windhagen, H., Meyer-Lindenberg, A., 2009. Comparison of the resorbable magnesium alloys LAE442 und MgCa0.8 concerning their mechanical properties, their progress of degradation and the bone-implant-contact after 12 months implantation duration in a rabbit model, *Materialwissenschaft und Werkstofftechnik* 40, p. 82.
- [8] Von Der Höh, N., Bormann, D., Lucas, A., Denkena, B., Hackenbroich, C., Meyer-Lindenberg, A., 2009. Influence of different machining treatments of magnesium-based resorbable implants on the degradation behavior in rabbits, *Advanced Engineering Materials* 11, p. B47.
- [9] Wang, H., Estrin, Y., Zúberová, Z., 2008. Bio-corrosion of a magnesium alloy with different processing histories, *Materials Letters* 62, p. 2476.
- [10] Denkena, B., Lucas, A., 2007. Biocompatible magnesium alloys as absorbable implant materials – adjusted surface and subsurface properties by machining processes, *CIRP Annals - Manufacturing Technology* 56, p. 113.
- [11] Guo, Y.B., Sealy, M.P., 2012. Significant improvement of corrosion resistance of biodegradable metallic implants processed by laser shock peening, *CIRP Annals - Manufacturing Technology* 61/1, p. 583.